Butyrate attenuates high-fat diet induced glomerulopathy through GPR43-Sirt3 pathway

Ying Shi[1], Lin Xing[1], Ruoyi Zheng[1], Xin Luo[1], Fangzhi Yue[1], Xingwei Xiang[1], Anqi Qiu[1], Junyan Xie[1], Ryan Russell[2], Dongmei Zhang[1,3*]

[1]Department of Endocrinology, Xiangya Hospital, Central South University, Changsha, China. [2]Department of Health and Human Performance, College of Health Professions, University of Texas Rio Grande Valley, Brownsville, Texas. [3]Hunan Engineering Research Center for Obesity and its Metabolic Complications, Xiangya Hospital, Central South University, Changsha, China.

Correspondence: *Dongmei Zhang, PhD, MD, Department of Endocrinology, Xiangya Hospital, Central South University, 87 Xiangya Road, Changsha 410008, China. Tel: (86) 731-89753727. Fax: (86) 731-84327166. E-mail: drdmzhang@csu.edu.cn

10.1017/S0007114524002964

The British Journal of Nutrition is published by Cambridge University Press on behalf of The Nutrition Society

Abstract

The incidence of obesity related glomerulopathy (ORG) is rising worldwide with very limited treatment methods. Paralleled with the gut-kidney axis theory, beneficial effects of butyrate, one of short-chain fatty acids produced by gut microbiota, on metabolism and certain kidney diseases have gained growing attention. However, the effects of butyrate on ORG and its underlying mechanism are largely unexplored. In this study, a mice model of ORG was established with high-fat diet (HFD) feeding for 16 weeks, and sodium butyrate treatment was initiated at the 8th week. Podocytes injury, oxidative stress, and mitochondria function were evaluated in mice kidney and validated *in vitro* in palmitic acid (PA) treated-MPC5 cells. Further, the molecular mechanisms of butyrate on podocytes were explored. Compared with controls, sodium butyrate treatment alleviated kidney injuries and renal oxidative stress in HFD-fed mice. In MPC5 cells, butyrate ameliorated PA-induced podocyte damage and helped maintain the structure and function of the mitochondria. Moreover, the effects of butyrate on podocytes were mediated *via* GPR43-Sirt3 signal pathway, as evidenced by the diminished effects of butyrate with the intervention of GPR43 or Sirt3 inhibitors. In summary, we conclude that butyrate has therapeutic potential for the treatment of ORG. It attenuates HFD-induced ORG and podocytes injuries through the activation of GPR43-Sirt3 signaling pathway.

Keywords: butyrate; mitochondria; obesity related glomerulopathy; podocytes.

Abbreviations:

ANOVA: one-way analysis of variance; ATP: adenosine triphosphate; AUC: areas under the curves; BUN: blood urea nitrogen; CCK-8: cell counting kit-8; CKD: chronic kidney disease; ESRD: end-stage renal disease; FFAR2: free fatty acid receptor 2; GSH: glutathione; HDL-c: high-density lipoprotein cholesterol; HE: hematoxylin and eosin; HFD: high-fat diet; IPGTT: intraperitoneal glucose tolerance test; ITT: insulin tolerance test; LDL-c: low-density lipoprotein cholesterol; MDA: malondialdehyde; MPC5: mouse podocyte cell line; ORG: obesity-related glomerulopathy; PAS: periodic acid-schiff; RAAS: renin-angiotensin-aldosterone system; ROS: reactive oxygen species; SCFAs: short-chain fatty acids; Scr: serum creatinine; TC: total cholesterol; TEM: transmission electron microscopy; TG: triglyceride; T-SOD: total superoxide dismutase; UA: uric acid; WT-1: Wilm’s tumor 1

Introduction

The obesity epidemic has led to an increased incidence of obesity-related glomerulopathy (ORG), which is pathologically characterized by glomerular basement membrane thickening, podocyte injury, glomerular hypertrophy and focal segmental glomerulosclerosis, resulting in proteinuria and progressive loss of renal function(1). About 30% of ORG patients develop progressive renal failure or end-stage renal disease (ESRD). Despite considerable efforts to characterize the pathophysiology of ORG, therapeutic approaches are very limited. Renin–angiotensin–aldosterone system (RAAS) inhibition and weight loss are the only two methods that are proven effective, but RAAS inhibitors have contraindications and their nephroprotective effects on ORG may be short-term, while weight loss is often challenging for patients with obesity(2). Therefore, exploring alternative or additive therapies is necessary for the improvement of kidney prognosis in ORG.

The relationship between gut microbiota and chronic kidney diseases is referred to as the "gut–kidney axis"(3). In recent years, a link between a contraction of short-chain fatty acids (SCFAs)-producing bacteria and kidney diseases has been proposed. SCFAs, mainly acetate, propionate and butyrate, are the end products of the fermentation of dietary fibers by the gut microbiota(4). Consumption of high dietary total fiber intake is associated with lower risk of inflammation and all-cause mortality in patients with chronic kidney diseases (CKD)(5). Consistently, reduced SCFAs-producing bacteria is observed in ESRD patients(6). Germ-free mice, which have very low levels of SCFAs, are more susceptible to renal injury, whereas conventionalization with bacteria in diet confers protection against renal injuries(7,8).

Among the SCFAs, butyrate stands out because it might have a potential in alleviating obesity and related metabolic complications(9). For demonstration, a lower abundance of butyrate-producing microbes in humans has been associated with an increased risk of metabolic disease, showing its strength in mitigation of the metabolic disturbances of obesity(10). Actually, a couple of studies have reported beneficial effects of butyrate on high fat diet (HFD)-induced obesity and glucolipid metabolism(11,12). Regarding its renal effects, butyrate has been shown to be able to ameliorate kidney oxidative damage, inflammation, apoptosis, fibrosis, pathological changes, and proteinuria in animal models of ischemia-reperfusion injury, diabetic nephropathy and immune-related chronic kidney disease(13-15). However, the mechanism of butyrate on the kidney diseases and whether it have a renoprotective effect on ORG remain to be elucidated.

Mitochondrial damage and dysfunction have been identified to play a critical role in the occurrence of ORG. Mitochondrial fragmentation, decreased adenosine triphosphate (ATP) content, and increased production of mitochondrial reactive oxygen species (ROS) are observed in kidney of HFD-fed mice and ob/ob mice(16,17). And mitochondria-targeted therapy, e.g. SS31, has been demonstrated to be beneficial for preventing renal damages induced by a HFD(18). These results highlight that targeting mitochondria may offer a potential strategy for the treatment of ORG. Previous studies have shown that butyrate improves kidney mitochondrial function in db/db diabetic mice, but the underlying mechanism remain largely unknown (19). In-depth investigation into the molecular mechanism on its effects on mitochondrial biology and pathology is essential to the discovery of more specific and efficacious approaches to target mitochondria for renoprotection.

The present study observed the effects of butyrate on proteinuria, kidney pathological changes, podocytes damages, and mitochondrial dysfunction in mice ORG model induced by HFD feeding, and explored the underlying molecular mechanisms involved in palmitic acid (PA) treated-MPC5 cells *in vitro.* Our present findings indicated the use of butyrate may hold promise for the prevention and treatment of ORG.

Materials and Methods

1. Ethical statement

All animal experiments in this study were conducted with the approval of the Animal Ethnics Committee of the Xiangya Medical Collage of Central South University (NO.2021sydw0119).

2. Animals

Five-week-old male C57BL/6 mice were obtained from the Hunan SJA Experimental Animal Company (Changsha, China). After a one-week acclimation, the mice were fed normal chow diet (12% fat, 22% protein and 66% carbohydrate, 3.5 kcal/g) or HFD (60% fat, 20% protein and 20% carbohydrate, 5.24 kcal/g, purchased from Research Diets, Inc.) for 16 weeks. After the initial 8 weeks' feeding, normal chow diet fed mice and HFD-fed mice received either sterilized vehicle (NC group or HC group, n=8) or sodium butyrate (NaB, Sigma-Aldrich 303410, 300 mg/kg/d) (NB group or HB group, n=8) by gavage once daily for the subsequent 8 weeks(20). Body weight and food intake were recorded weekly. At the end of the 16th week, mice were fasted overnight and then sacrificed. Blood samples were harvested for biochemical analysis. After isolation of the kidneys, a transverse slice was fixed in 4% paraformaldehyde, and portions of kidney cortex were fixed with 2.5% glutaraldehyde for subsequent pathological and transmission electron microscopy analysis. Remaining kidney tissue was frozen at -80℃ until further analysis. All animals were housed under a 12-hour light/dark cycle at constant temperature.

3. Cell culture

A conditionally immortalized mouse podocyte cell line (MPC5) was purchased from BeNa Culture Collection (Jiangsu Province, China) and cultured as described previously(21). Briefly, podocytes were grown in RPMI-1640 medium (Gibco) supplemented with 10% fetal bovine serum (Gibco) and mouse recombinant interferon-gamma (IFN-γ, Sigma-Aldrich, 10U/ml) at 33℃, and subsequently differentiated in RPMI-1640 without IFN-γ at 37℃. PA solution was prepared as described previously(22). Briefly, PA powder (Sigma-Aldrich, P0500) was dissolved in DMSO to a concentration of 10mM. PA was then conjugated in DMEM with 1% fatty acid-free BSA to a final concentration of 0.3mM. Podocytes were incubated with 0.3mM PA for 24 hours(23), and subsequently treated with or without sodium butyrate (But) (1mM, APExBIO, B1835), or 3-TYP (TYP, the inhibitor of Sirt3) (50μM, TOPSCIENCE, T4108), or GLPG0974 (GLPG, the inhibitor of GPR43) (10μM, R＆D Systems, 5621/10) for another 24 hours, and then cells were lysed for mRNA and protein analysis.

4. Urinary albumin determination

24 hours of urine excretion was collected using metabolic cages at the 12th and 16th week. Urinary albumin levels were measured by mouse microalbuminuria ELISA kit (JL20486, Jianglaibio) according to the manufacturer's instructions.

5. Intraperitoneal glucose tolerance test (IPGTT) and insulin tolerance test (ITT)

IPGTT and ITT were performed at the 15th week. Mice were fasted overnight prior to the IPGTT or 5 hours prior to the ITT. Glucose levels were measured sequentially from the tail vein at 0, 30, 60 and 120 min, after intraperitoneally injection of either glucose (2g/kg bodyweight) or insulin (0.5UI/kg bodyweight). Areas under the curves (AUC) for IPGTT and ITT were calculated to evaluate glucose tolerance and insulin tolerance.

6. Biochemical assays

Blood urea nitrogen (BUN), serum creatinine (Scr), uric acid (UA), triglycerides (TG), total cholesterol (TC), low-density lipoprotein cholesterol (LDL-c), and high-density lipoprotein cholesterol (HDL-c) were measured by commercial reagents (Serotec Co., Sapporo, Japan) on an automatic biochemical analyzer (Hitachi, Tokyo, Japan) according to the manufacturer's recommendations.

7. Serum butyrate measurement

Serum butyrate were measured using HPLC-MS/MS method as previously described (24). Briefly, butyrate was extracted from serum samples using acetonitrile and derivatized with 3-nitrophenylhydrazine, then were analyzed on a Jasper HPLC coupled to a Sciex 4500 MD system. Octanoic acid-1-13C1 (Sigma-Aldrich, 605832) and Butyric-2,2-d2 (CDN Isotopes, 19136-92-6) were used as internal standards.

8. Serum 3-hydroxybutyrate assay

3-hydroxybutyrate levels were measured by an enzymatic 3-hydroxybutyrate dehydrogenase-based assay kit (MEIKANG Bio Inc) according to the manufacturer's instructions.

9. Histology staining

Kidneys were fixed in 4% paraformaldehyde and then embed in paraffin (4 μm thickness). Sections were stained with hematoxylin and eosin (HE) or periodic acid-schiff (PAS) or masson trichrome. All tissue assessments were performed in a blinded fashion. Semi-quantitative evaluation was performed with Image J software.

10. Immunohistochemical and immunofluorescence staining

Immunohistochemical staining was performed with paraffin-embedded kidney tissues. Sections were deparaffinized and heated in citrate buffer for 20 minutes for antigen retrieval, and then sequentially incubated with peroxide and goat serum for blocking. The sections were then incubated with anti-Wilm's tumor 1 (WT-1) antibody (Abcam, ab267377) at 4℃ overnight and subjected to immunohistochemical analysis.

Frozen kidney sections were used for immunofluorescence staining. After the slices were incubated with anti-WT1 antibody, or anti-GPR43 antibody (Proteintech, 19952-1-AP), or anti-Sirt3 antibody (Abcamab, 246522) overnight at 4℃, an IgG antibody conjugated to fluorescein was used as a secondary antibody. Nuclei were stained with DAPI and images were captured using Leica DM2500 fluorescence microscopy.

11. Transmission electron microscopy (TEM)

Kidney cortex or podocytes were fixed in 2.5% glutaraldehyde and embedded in resin according to standard procedures. Ultrathin sections were stained with uranyl acetate/lead citrate, and examined under an electron microscope (JEOL, JEM1400).

12. Western blot analysis

The renal cortex tissues or podocytes samples were lysed in RIPA lysis buffer. Subsequently, denatured proteins were separated by SDS-PAGE electrophoresis and transferred to a PVDF membrane (Merck Millipore). After blocking by BSA solution for 1 hour, the membranes were then incubated with primary antibodies overnight at 4℃, followed by corresponding horseradish peroxidase-conjugated antibody for 1 hour and detection by chemiluminescence. The primary antibodies used were as follows: anti-GAPDH (Proteintech, 10494-1-AP), anti-beta actin (Proteintech, 81115-1-RR), anti-WT-1 (Abcam, ab267377), anti-PGC1-alpha (Proteintech, 66369-1-Ig), anti-GPR43 (Proteintech, 19952-1-AP), and anti-Sirt3 (Abcamab, 246522). Quantification was performed by measuring the gray value with the Image Lab software.

13. Real-time RT-PCR

Total RNA was extracted from kidney or podocytes with Total RNA Isolation Kit (Foregene, RE-03011/03111), and reverse-transcribed into cDNA using HiFiScript cDNA Synthesis Kit (CWBIO, CW2569M) following the manufacturer’s protocol. The cDNA samples were diluted 20-fold, and real-time PCR reaction was carried out using SYBR Green PCR Pre-mixed Solution (Thermo Fisher, 4309155). Amplifications were performed in a QuantStudio 7 Real-Time PCR System (Thermo Fisher Scientific). All standards and samples were assayed in triplicate. The sequences of the primer pairs are listed in Table S1.

14. Assay of oxidant markers

Kidney cortex and podocytes lysates were collected for estimating malondialdehyde (MDA), glutathione (GSH) and total superoxide dismutase (T-SOD), by using each Assay Kit (Nanjing Jiancheng, A003-1-2 / A006-1-1 / A001-1-2) according to the manufacturer’s recommendations.

15. Cell viability assessment

The viability of MPC5 cells was determined using a Cell Counting Kit-8 (CCK-8) (TOPSCIENCE, C0005). Briefly, cells were inoculated onto a 96-well plate and incubated with different concentrations of PA or butyrate for 24 hours or 48 hours. Then, 10μl per well

CCK-8 solution was added to the culture medium, and the absorbance value was measured at 450nm. Results were shown as the percentage of CCK-8 reduction, and the absorbance of control group was set at 100%.

16. ATP assay

ATP levels were measured using ATP Assay Kit (Beyotime, S0026) according to the manufacturer's protocol. Briefly, podocytes lysates were centrifuged at 12,500 × g for 5 minutes at 4℃ to get the supernatants. Treated samples were mixed with ATP reaction mix in 96-well plates and the luminescence was measured by LuminMaxC Luminometer (Promega, GLOMAX-MULTI).

17. ROS assay

ROS generation was detected by ROS assay kit (Beyotime, S0033S) according to the manufacturer's instructions. Podocytes were seeded into 6-well plates, and after various treatment conditions, cells were incubated with fluorescent probe DCFH-DA for 20 minutes at 37℃. Then the fluorescence intensity was examined with a flow cytometer (Attune CytPix, Thermo Fisher) to assess ROS generation.

18. Mito-Tracker staining

Mitochondria were stained by fluorescent probe Mito-Tracker Green (Beyotime, C1048). After each treatment condition, podocytes were incubated with Mito-Tracker Green for 30 minutes at 37℃. Images were taken under a fluorescence microscope (Leica, DM2500). Two replicates were performed for each biological sample.

19. Statistical analysis

Data are presented as mean ± SEM. Statistical analysis was performed using the IBM SPSS Statistics 22.0. For normally distributed data, the differences among groups were evaluated by a one-way analysis of variance (ANOVA) followed by the Bonferroni post hoc test (assuming equal variances) or Tamhane's T2 post hoc test (without the assumption of equal variances). Kruskal-Wallis test with Dunn's test was used for non-normally distributed data. P values less than 0.05 were considered statistically significant.

Results

1. Sodium butyrate ameliorated HFD-induced metabolic disorders.

The HC group had increased body weight than the NC group. The HB group exhibited lower body weight than the HC group from the 13th week onwards, and no difference in food intake was noted between HC and HB groups (Figure 1a, b). Compared with the NC group, the HC group demonstrated impaired glucose tolerance and insulin sensitivity, increased visceral fat and higher serum TC, LDL-c, HDL-c levels. HB mice exhibited alleviated glucose tolerance and improved insulin sensitivity and decreased serum TC level in comparison to HC group (Figure 1c-f). There was a decreased tendency of relative visceral fat weight in the HB group *vs.* the HC group ($p = 0.06$) (Figure 1e). There were no significant differences in body weight, glucolipids, insulin resistance between NC and NB groups (Figure 1a-f).

2. Serum butyrate and 3-hydroxybutyrate.

Compared with ND-fed mice, HFD-fed mice had significantly decreased concentration of serum butyrate. And butyrate gavage led to significant increases in serum butyrate in both ND-fed and HFD-fed mice (Figure 2a).

Butyrate was also rapidly metabolized by the liver to 3-hydroxybutyrate, which might have beneficial effects on organismal metabolism. For this reason, we also measured the levels of serum 3-hydroxybutyrate. The results showed that levels of 3-hydroxybutyrate significantly increased in HFD-fed mice, but were not impacted by butyrate treatment in both ND-fed and HFD-fed mice (Figure 2b).

3. Sodium butyrate administration prevented HFD-induced kidney injury.

HFD led to renal dysfunction, as evidenced by increased serum creatinine levels and urinary albumin excretion in HC mice. Compared with the HC group, HB group had decreased serum creatinine and urinary albumin excretion (Figure 3a, b). Pathologically, HC mice displayed increases in glomerular diameter and deposition of glycogen and collagen fibers in the glomerular region, while HB mice exhibited less glomerulomegaly, mesangial expansion and renal fibrosis (Figure 3c-e).

Collectively, these data indicated that butyrate ameliorated HFD-induced obesity, insulin resistance, glucolipid dysmetabolism and renal injuries in mice.

4. Sodium butyrate administration ameliorated HFD-induced podocytes damage.

Given the crucial roles of podocytes in the maintenance of the structure and filtration capacity of glomeruli(25), we then assessed the impacts of butyrate on podocyte damage. TEM revealed that podocytes in HC mice had irregular shape with diffuse foot process fusion and glomerular basement membrane thickening, and butyrate treatment led to improvements in podocytes foot process effacement and reduced glomerular basement membrane (Figure 4a). Also, we detected podocyte density by immunohistochemical staining of WT-1, the marker for podocytes. Compared with NC mice, podocyte density in glomerular area of the HC mice was significantly decreased, assessed by WT-1 positive area, and increased in HB group *vs.* HC group, these results were further confirmed by western blot analysis of renal cortex (Figure 4b, c).

To clarify whether there were direct effects of butyrate on the podocytes, we conducted the *in vitro* experiments in MPC5 cells. To mimic podocytes damage of HFD-induced renal injury, we treated cultured MPC5 cells with PA. According to CCK-8 cell viability assay, cell viability was decreased with 0.3mM PA treatment, and treatment with 1.0mM butyrate significantly increased cell viability in PA-treated MPC5 cells (Figure S1a-c). Thus, we selected 0.3mM PA and 1.0mM butyrate for the following experiments (19, 23).

Consistent with *in vivo* results, expressions of WT-1, nephrin, and podocin were significantly decreased with PA treated MPC5 cells, and butyrate increased the expressions of these podocyte markers (Figure 4d, e).

5. Sodium butyrate partially reversed HFD-induced oxidative stress and mitochondrial damage.

Since oxidative stress and mitochondrial dysfunction are key molecular events in the pathogenesis of ORG(26), we then explored effects of sodium butyrate on oxidative stress and mitochondrial damage *in vivo* and *in vitro.* HC mice had lower GSH and higher MDA in renal tissues *vs.* NC mice. Compared with HC mice, HB mice had lower MDA in renal tissues (Figure 5a, b). TEM revealed mitochondrial swelling and cristae fracture or loss in HC mice, and these changes were ameliorated in HB mice (Figure 5c).

In PA-treated MPC5 cells, there were decreases in antioxidant scavengers such as T-SOD and GSH, and an increase in ROS. Butyrate intervention led to increases in T-SOD and GSH and a decrease in ROS (Figure 5d-f).

Effects of sodium butyrate on mitochondrial were also observed in MPC5 cells *in vitro*. We found that expression of Nrf-1, TFAM, PGC-1α and electron transporter chain-related genes (Ndufa1, COX Ⅳ, ATP5o) were downregulated by PA stimulation, while butyrate intervention upregulated expression of these genes, indicating increased mitochondrial biogenesis and mitochondrial integrity of podocytes with butyrate treatment (Figure 5g, Figure S2a, b). ATP levels were measured to assess the effect of butyrate on mitochondrial function. ATP levels were decreased in PA-treated MPC5, and were better preserved after butyrate intervention (Figure 5h). Further, we analyzed mitochondrial mass by Mito-Tracker staining and the ultrastructural of mitochondria using electron microscopy. Mitochondrial mass was significantly lower with PA stimulation, while treatment with butyrate largely preserved mitochondrial mass (Figure 5i). And TEM analysis displayed PA-treated MPC5 cells with swollen mitochondria and disorganized and fragmented cristae, while butyrate intervention preserved a relatively normal structure of mitochondria (Figure 5j). Collectively, these results showed that butyrate improved the morphology and function of podocytes mitochondria.

6. Sodium butyrate ameliorated podocytes injury *via* the activation of GPR43-Sirt3 pathway

GPR43 is one of the main receptors for SCFAs(27). Here we found that GPR43 expressed and co-localized with WT-1 in the glomerular region of kidney in mice by double immunofluorescent staining, indicating that GPR43 is present in podocytes (Figure 6a). The expression of WT-1 and GPR43 were decreased in renal tissue of the HC group *vs.* the NC group, while the HB group had increased WT-1 and GPR43 expressions *vs*. the HC group. Western blot further confirmed this result (Figure 6a, b). Consistently, our data shows that protein levels of GPR43 were downregulated upon exposure to PA in MPC5 cells, and were upregulated by butyrate treatment (Figure 6d). To further elucidate whether GPR43 is involved in the protective effect of butyrate on podocytes, we downregulated GPR43 by GLPG0974, an antagonist of GPR43, and found GLPG0974 overrode butyrate-mediated increases in WT-1 and PGC-1α protein in podocytes (Figure 4e, 5g). Moreover, GLPG0974 effectively blocked the butyrate-mediated increases of T-SOD and GSH as well as ATP production in MPC5 cells, suggesting that the protective effects of butyrate on podocytes were GPR43-dependent (Figure 5d, e, h).

Next, we explored possible signaling molecules involved in the protective effects of butyrate on podocytes. Sirt3 is a crucial metabolic sensor that regulates mitochondrial homeostasis(28). As revealed by immunofluorescent staining assays, glomerular expression of Sirt3 was lower in HFD-fed mice, and butyrate supplementation markedly recovered its expression (Figure 6c). In PA-treated MPC5 cells, downregulated Sirt3 was restored by butyrate, and both GLPG0974 and 3-TYP (the inhibitor of Sirt3) suppressed the expression of Sirt3, while 3-TYP failed to affect GPR43 expression, indicating that Sirt3 acts downstream of GPR43 (Figure 6d). Further, 3-TYP treatment inhibited butyrate-induced increases in expression of WT-1, PGC-1α, and levels of ATP, T-SOD and GSH in MPC5 cells (Figure 4e, Figure 5d, e, g, h). Taken together, these results suggested that GPR43-Sirt3 pathway was involved in the renal protective effects of butyrate.

Discussion

Obesity is regarded as a major and independent risk factor for the development of CKD. With the increased prevalence of obesity worldwide, ORG has become a global issue(29). A retrospective study that evaluated native kidney biopsy samples received at Columbia University reported a 10-fold increase in the incidence of ORG from 0.2% in 1986–1990 to 2.0% in 1996–2000, with a further rise to 2.7% in 2001–2015(1,30). Further, a recent study in

China showed that the annual incidence of ORG increased from 0.86% in 2009 to 1.65% in 2018(31). However, there are currently limited effective treatment options for ORG. Here, paralleled with the gut-kidney axis theory, our experiments suggest that butyrate, an intestinal metabolite, prevents proteinuria, glomerulomegaly, mesangial expansion and renal fibrosis in HFD-fed mice, indicating its protective effects on ORG. Podocyte dysfunction is a prominent mediator in the pathogenesis of ORG(1). Also, we found that butyrate increased podocyte density and improved its morphology and function *in vivo* and *in vitro*. To the best of our knowledge, this is the first report that explored effects of butyrate on ORG.

Metabolic dysfunction, such as hyperlipidemia and insulin resistance contribute to renal injury in ORG(26). Insulin resistance leads to glomerular hyperfiltration and excessive sodium reabsorption, ultimately causing renal damage, endothelial dysfunction, increased vascular permeability, and renal hypertrophy(32). Lipid overload causes mitochondria damage and decreased AMPK activity, resulting in podocyte apoptosis(33). Our data demonstrated the beneficial effects of butyrate on metabolic dysfunction in HFD mice without significant impact on food intake, indicating the protective effects of butyrate on ORG are associated with its metabolic effects.

Kidneys are organs with continuous high-energy consumption. Mitochondrial injury plays a critical role in HFD-induced podocytes damage(18). Here, we found that sodium butyrate supplementation inhibited oxidative stress and ameliorated mitochondrial damage in the kidney of HFD mice. Also, in PA-induced MPC5, our data confirmed that butyrate increased mitochondrial biogenesis, maintained the integrity of the mitochondrial electron transport chain, and protected mitochondrial function in podocytes. Roles of butyrate in regulating mitochondrial biogenesis has been reported in both skeletal muscle and brown adipose tissue(11,33). The present experiment provided the first evidence illustrating the effects of butyrate on mitochondrion in podocytes.

GPR43, also known as free fatty acid receptor 2 (FFAR2), is one of the primary receptors for butyrate. The involvement of GPR43 in mechanism of butyrate on kidney diseases has been suggested. Huang W *et al.* reported that butyrate inhibited renal fibrosis and mesangial matrix accumulation in diabetic nephropathy *via* GPR43-mediated inhibition of oxidative stress(34). Of note in our experiment, GPR43 was demonstrated to be expressed in podocytes, and that butyrate markedly increased the expression of GPR43 in HFD mice kidney and podocytes *in vitro*. In addition, the protective effects of butyrate on podocytes were compromised by GPR43 inhibitor, suggesting that GPR43 is required for butyrate to exert a nephroprotective effect.

We then sought to elucidate the molecular effects downstream of GPR43. Sirt3 is known to regulate mitochondrial oxidative stress, and is linked to kidney diseases (28). Wang Q *et al.* reported that Sirt3 overexpression alleviated renal ischemia-reperfusion injuries through enhancing mitochondrial fusion(35). Our results show that butyrate upregulated the expression of Sirt3 in PA-induced MPC5 cells and that mitochondrial-protective effects of butyrate were significantly offset by Sirt3 antagonist, supporting the notion that Sirt3 plays a critical role in the actions of butyrate on mitochondrial homeostasis in podocytes. Further, GPR43 inhibitor decreased the expression of both GPR43 and Sirt3, indicating that Sirt3 may act as a mediator downstream of GPR43. Given the renoprotective activity of Sirt3 in counteracting mitochondrial dysfunction in podocytes, Sirt3-activator compounds, such as silybin, resveratrol and curcumin, may have a renoprotective effect on ORG.

Interestingly, our results showed concentration of serum butyrate in mice was about 1μM~10μM, which is much lower than that we used in the MPC5 experiments (1.0mM). The major discrepancy can be explained by several reasons. Firstly, there are big difference between *in vitro* experiment and *in vivo* study. The *in vitro* tests are not the same as actual cells or tissues and used to simulate the real phenomenon. Secondly, we used MPC5 cell lines, a conditionally immortalized mouse podocyte clone(36) . Such transformed cells may not act like normal physiological cells, so that we could not expect the normal physiological response to butyrate. Thirdly, the distribution of butyrate varies among different tissues (24). For these reasons, it is inaccurate to extrapolate the dose levels we used in the MPC5 experiments to physiological butyrate levels. Nevertheless, the MPC5 experiments assist to discover the underlying molecular mechanisms of butyrate.

This study is not without limitations. Previous studies have shown beneficial effects of butyrate on several renal diseases, with butyrate dose range from 100mg/kg/48h to 1g/kg/day(34,37). Our study adopted a single dose of 300mg/kg/day and found a renoprotective effect on ORG. Further researches are needed to determine whether there is a dose-dependent effect of butyrate on ORG. Furthermore, in addition to activating G protein-coupled receptors, butyrate also acts as an important regulator of histone acetylation and promotes histone acetylation by inhibiting histone deacetylase. It has been reported that butyrate prevents obesity-induced cognitive impairment by epigenetically enhancing H3K18ac(38). Here our study discovered the involvement of GPR43 in mechanism of butyrate on ORG, whether the epigenetic mechanisms are also involved in the renoprotective effect of butyrate remain to be explored.

In conclusion, this study identified a novel mechanism that butyrate regulated mitochondrial function and protected podocytes injury *via* GPR43-Sirt3 signaling pathway. These findings also suggest that therapeutic approaches, such as butyrate and other Sirt3 activators targeting podocytes, may have potential for the treatment of ORG. On the other hand, the renoprotective effect of butyrate, one of SCFAs produced by gut microbiota, also revealed a close connection between the gut and the kidney. Therefore, interventions aimed at regulating metabolites of gut microbiota may provide therapeutic strategies for the treatment of ORG.

Author Contributions

YS: Methodology, Investigation, Writing-Original Draft; **LX**: Investigation; **RZ**: Investigation; **XL**: Investigation; **FY**: Methodology; **XX**: Methodology; **AQ**: Methodology; **JX**, Methodology; **RR**: Writing-Review & Editing; **DZ**: Conceptualization, Writing-Review & Editing, Funding acquisition.

Grants

The work is supported by National Natural Science Foundation of China (NO.82070884) and Natural Science Foundation of Hunan Province (No. 2024JJ5550).

Competing Interests

The authors declare that they have no financial/commercial conflicts of interest.

Data Availability

The datasets used and/or analyzed during the current study are available from the corresponding author on reasonable request.

References

1. D'Agati VD, Chagnac A, de Vries AP *et al*. (2016) Obesity-related glomerulopathy: clinical and pathologic characteristics and pathogenesis. *NAT REV NEPHROL* **12**, 453-471.

2. Martinez-Montoro JI, Morales E, Cornejo-Pareja I *et al*. (2022) Obesity-related glomerulopathy: Current approaches and future perspectives. *OBES REV* **23**, e13450.

3. Stavropoulou E, Kantartzi K, Tsigalou C *et al*. (2020) Focus on the Gut-Kidney Axis in Health and Disease. *Front Med (Lausanne)* **7**, 620102.

4. van der Hee B, Wells JM. (2021) Microbial Regulation of Host Physiology by Short-chain Fatty Acids. *TRENDS MICROBIOL* **29**, 700-712.

5. Su G, Qin X, Yang C *et al*. (2022) Fiber intake and health in people with chronic kidney disease. *Clin Kidney J* **15**, 213-225.

6. Wong J, Piceno YM, DeSantis TZ *et al*. (2014) Expansion of urease- and uricase-containing, indole- and p-cresol-forming and contraction of short-chain fatty acid-producing intestinal microbiota in ESRD. *AM J NEPHROL* **39**, 230-237.

7. Campbell C, Kandalgaonkar MR, Golonka RM *et al*. (2023) Crosstalk between Gut Microbiota and Host Immunity: Impact on Inflammation and Immunotherapy. *Biomedicines* **11**.

8. Gharaie S, Lee K, Newman-Rivera AM *et al*. (2023) Microbiome modulation after severe acute kidney injury accelerates functional recovery and decreases kidney fibrosis. *KIDNEY INT* **104**, 470-491.

9. Coppola S, Avagliano C, Calignano A *et al*. (2021) The Protective Role of Butyrate against Obesity and Obesity-Related Diseases. *MOLECULES* **26**.

10. Stoeva MK, Garcia-So J, Justice N *et al*. (2021) Butyrate-producing human gut symbiont, Clostridium butyricum, and its role in health and disease. *Gut Microbes* **13**, 1-28.

11. Hong J, Jia Y, Pan S *et al*. (2016) Butyrate alleviates high fat diet-induced obesity through activation of adiponectin-mediated pathway and stimulation of mitochondrial function in the skeletal muscle of mice. *Oncotarget* **7**, 56071-56082.

12. Peng K, Dong W, Luo T *et al*. (2023) Butyrate and obesity: Current research status and future prospect. *Front Endocrinol (Lausanne)* **14**, 1098881.

13. Sun Y, Zhou C, Chen Y *et al*. (2022) Quantitative increase in short-chain fatty acids, especially butyrate protects kidney from ischemia/reperfusion injury. *J Investig Med* **70**, 29-35.

14. Yang T, Li L, Heng C *et al*. (2024) Sodium butyrate ameliorated diabetic nephropathy-associated tubulointerstitial inflammation by modulating the tight junctions of renal tubular epithelial cells. *FOOD FUNCT* **15**, 2628-2644.

15. Liu J, Gu QH, Cui Z *et al*. (2024) Short-chain fatty acids ameliorate experimental anti-glomerular basement membrane disease. *CLIN IMMUNOL* **259**, 109903.

16. Prem PN, Kurian GA. (2021) High-Fat Diet Increased Oxidative Stress and Mitochondrial Dysfunction Induced by Renal Ischemia-Reperfusion Injury in Rat. *FRONT PHYSIOL* **12**, 715693.

17. Munusamy S, Do CJ, Hosler JP *et al*. (2015) Obesity-induced changes in kidney mitochondria and endoplasmic reticulum in the presence or absence of leptin. *Am J Physiol Renal Physiol* **309**, F731-F743.

18. Szeto HH, Liu S, Soong Y *et al*. (2016) Protection of mitochondria prevents high-fat diet-induced glomerulopathy and proximal tubular injury. *KIDNEY INT* **90**, 997-1011.

19. Yu Y, Jia YY, Li HJ. (2023) Sodium butyrate improves mitochondrial function and kidney tissue injury in diabetic kidney disease via the AMPK/PGC-1alpha pathway. *Ren Fail* **45**, 2287129.

20. Sun B, Jia Y, Hong J *et al*. (2018) Sodium Butyrate Ameliorates High-Fat-Diet-Induced Non-alcoholic Fatty Liver Disease through Peroxisome Proliferator-Activated Receptor alpha-Mediated Activation of beta Oxidation and Suppression of Inflammation. *J Agric Food Chem* **66**, 7633-7642.

21. Ni L, Saleem M, Mathieson PW. (2012) Podocyte culture: tricks of the trade. *Nephrology (Carlton)* **17**, 525-531.

22. Sweet DR, Vasudevan NT, Fan L *et al*. (2020) Myeloid Kruppel-like factor 2 is a critical regulator of metabolic inflammation. *Nat Commun* **11**, 5872.

23. Kaewin S, Changsorn K, Sungkaworn T *et al*. (2022) Fungus-Derived 3-Hydroxyterphenyllin and Candidusin A Ameliorate Palmitic Acid-Induced Human Podocyte Injury via Anti-Oxidative and Anti-Apoptotic Mechanisms. *Molecules* **27** (7).

24. Li B, Li L, Li M *et al.* (2019) Microbiota Depletion Impairs Thermogenesis of Brown Adipose Tissue and Browning of White Adipose Tissue. *CELL REP* **26**, 2720-2737.

25. Kopp JB, Anders HJ, Susztak K *et al*. (2020) Podocytopathies. *NAT REV DIS PRIMERS* **6**, 68.

26. Wei L, Li Y, Yu Y *et al*. (2021) Obesity-Related Glomerulopathy: From Mechanism to Therapeutic Target. *Diabetes Metab Syndr Obes* **14**, 4371-4380.

27. Kimura I, Ichimura A, Ohue-Kitano R *et al*. (2020) Free Fatty Acid Receptors in Health and Disease. *PHYSIOL REV* **100**, 171-210.

28. Morigi M, Perico L, Benigni A. (2018) Sirtuins in Renal Health and Disease. *J AM SOC NEPHROL* **29**, 1799-1809.

29. Xu T, Sheng Z, Yao L. (2017) Obesity-related glomerulopathy: pathogenesis, pathologic, clinical characteristics and treatment. *Front Med* **11**, 340-348.

30. Kambham N, Markowitz GS, Valeri AM *et al*. (2001) Obesity-related glomerulopathy: an emerging epidemic. *KIDNEY INT* **59**, 1498-1509.

31. Hu R, Quan S, Wang Y *et al*. (2020) Spectrum of biopsy proven renal diseases in Central China: a 10-year retrospective study based on 34,630 cases. *Sci Rep* **10**, 10994.

32. De Cosmo S, Menzaghi C, Prudente S *et al*. (2013) Role of insulin resistance in kidney dysfunction: insights into the mechanism and epidemiological evidence. *Nephrol Dial Transplant* **28**, 29-36.

33. Gao Z, Yin J, Zhang J *et al*. (2009) Butyrate improves insulin sensitivity and increases energy expenditure in mice. *DIABETES* **58**, 1509-1517.

34. Huang W, Man Y, Gao C *et al*. (2020) Short-Chain Fatty Acids Ameliorate Diabetic Nephropathy via GPR43-Mediated Inhibition of Oxidative Stress and NF-kappaB Signaling. *OXID MED CELL LONGEV* **2020**, 4074832.

35. Wang Q, Xu J, Li X *et al*. (2019) Sirt3 modulate renal ischemia-reperfusion injury through enhancing mitochondrial fusion and activating the ERK-OPA1 signaling pathway. *J CELL PHYSIOL* **23**4, 23495-23506.

36. Mundel P, Reiser J, Zuniga MBA *et al*. (1997) Rearrangements of the cytoskeleton and cell contacts induce process formation during differentiation of conditionally immortalized mouse podocyte cell lines. *EXP CELL RES* **236**, 248-258.

37. Du Y, Yang YT, Tang G *et al*. (2020) Butyrate alleviates diabetic kidney disease by mediating the miR-7a-5p/P311/TGF-beta1 pathway. *FASEB J* **34**, 10462-10475.

38. Ge X, Zheng M, Hu M *et al*. (2023) Butyrate ameliorates quinolinic acid-induced cognitive decline in obesity models. *J CLIN INVEST* **133**.

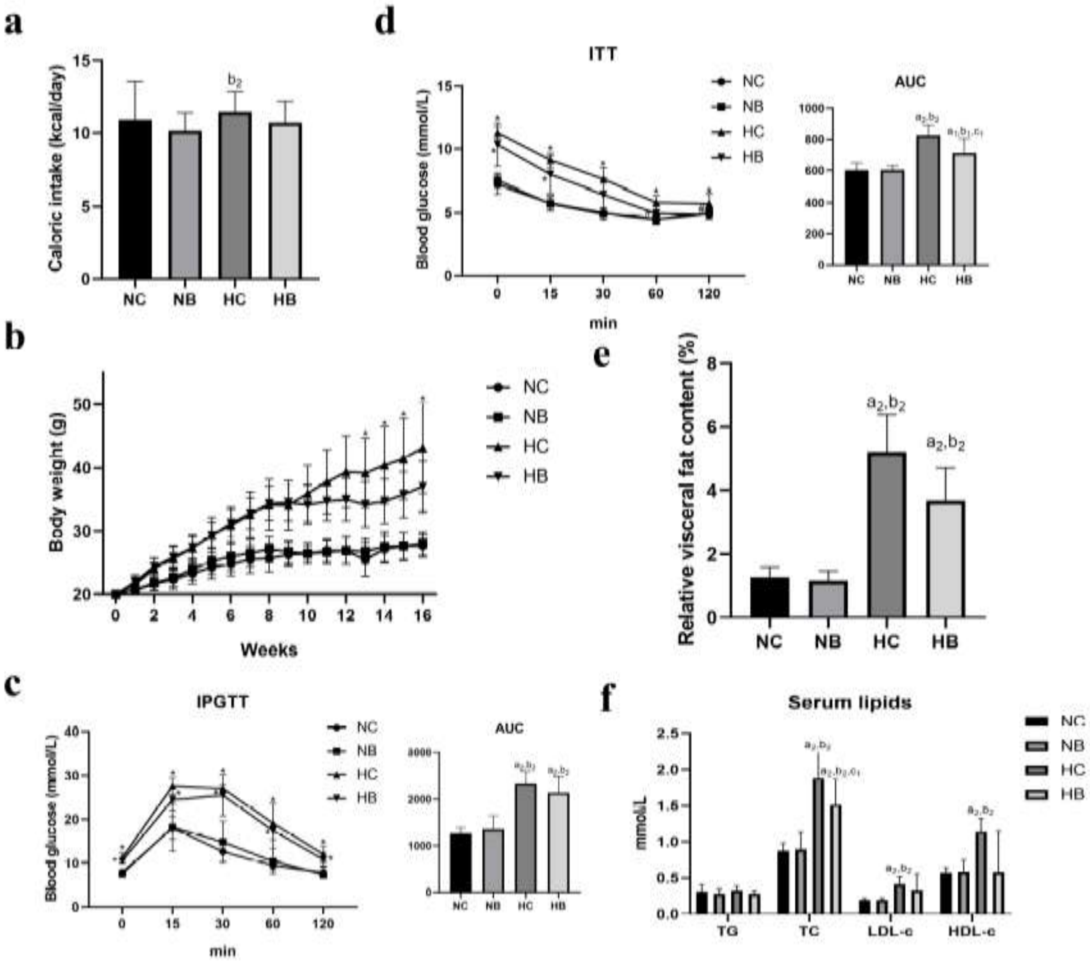

Figure 1. Sodium butyrate administration ameliorated HFD-induced metabolic disorders. **(a)** Caloric intake and **(b)** body weight of mice during 16 weeks' experiment. **(c)** Blood glucose levels during IPGTT and AUC analysis at week 15. IPGTT: intraperitoneal glucose tolerance test; AUC: area under curve. **(d)** Blood glucose levels during ITT and AUC analysis at week 15. ITT: insulin tolerance test. **(e)** Relative visceral fat content (visceral fat weight/body weight). **(f)** Serum lipids. TG: triglyceride; TC: total cholesterol; LDL-c: low-density lipoprotein cholesterol; HDL-c: high-density lipoprotein cholesterol. All values are shown as the means ± SEM. n=6-8 each group. **(a, c-f)** $^{a1}p<0.05$, $^{a2}p<0.01$ *vs.* NC group; $^{b1}p<0.05$, $^{b2}p<0.01$ *vs.* NB group; $^{c1}p<0.05$, $^{c2}p<0.01$ *vs.* HC group; **(b)** $*p<0.05$, $**p<0.01$ when HB group *vs.* HC group; **(c, d)** $*p<0.05$ *vs.* NC group; $\#p<0.05$ *vs.* HC group. Statistical significances were determined by one-way ANOVA.

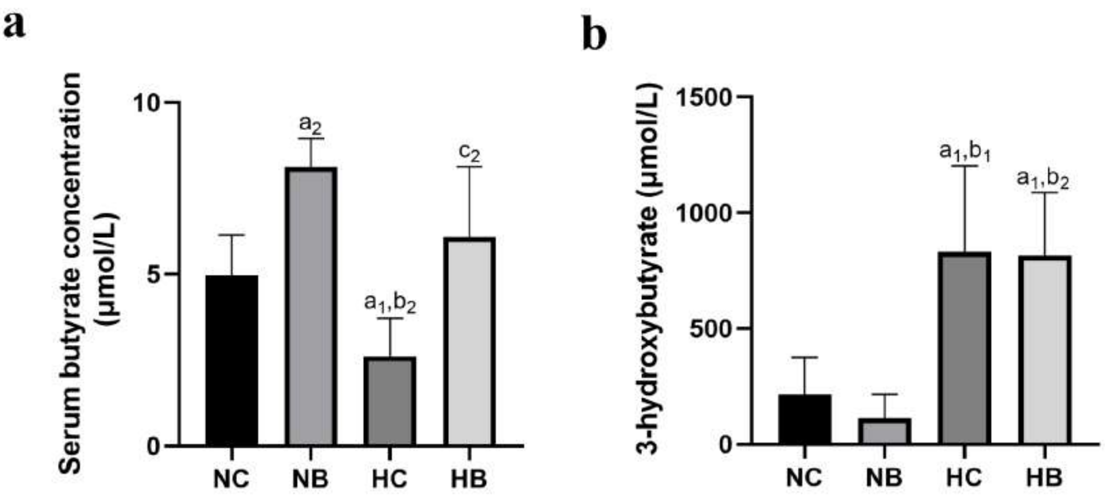

Figure 2. Serum butyrate and 3-hydroxybutyrate. **(a)** Serum butyrate levels. **(b)** Serum 3-hydroxybutyrate levels. **(a-b)** $^{a1}p<0.05$, $^{a2}p<0.01$ *vs.* NC group; $^{b1}p<0.05$, $^{b2}p<0.01$ *vs.* NB group; $^{c1}p<0.05$, $^{c2}p<0.01$ *vs.* HC group. Statistical significances were determined by one-way ANOVA.

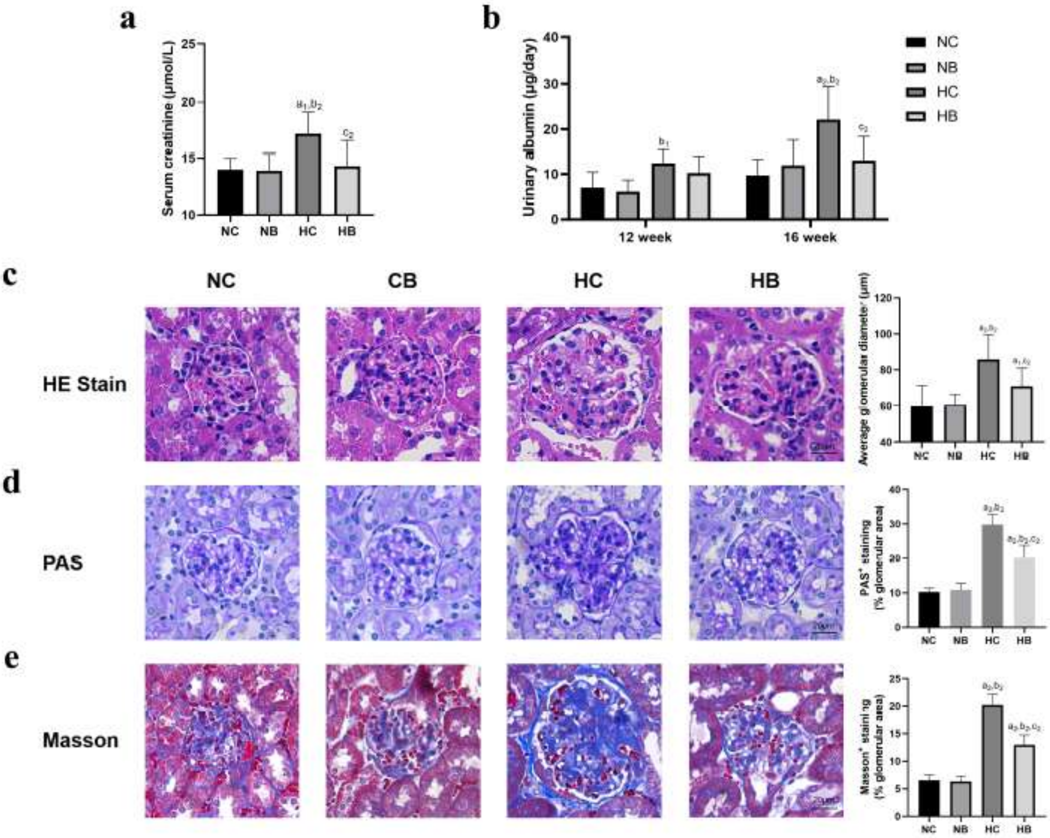

Figure 3. Sodium butyrate administration prevented HFD-induced kidney injury. **(a)** Serum creatinine levels. **(b)** Urinary albumin excretion levels at the 12th and 16th week. **(c)** Representative pictures of H&E staining, **(d)** PAS staining and **(e)** Masson staining of kidney tissue. Scale bars, 20μm. All values are shown as the means ± SEM. n=6-8 each group. **(a-d)** $^{a1}p<0.05$, $^{a2}p<0.01$ *vs.* NC group; $^{b1}p<0.05$, $^{b2}p<0.01$ *vs.* NB group; $^{c1}p<0.05$, $^{c2}p<0.01$ *vs.* HC group. Statistical significances were determined by one-way ANOVA.

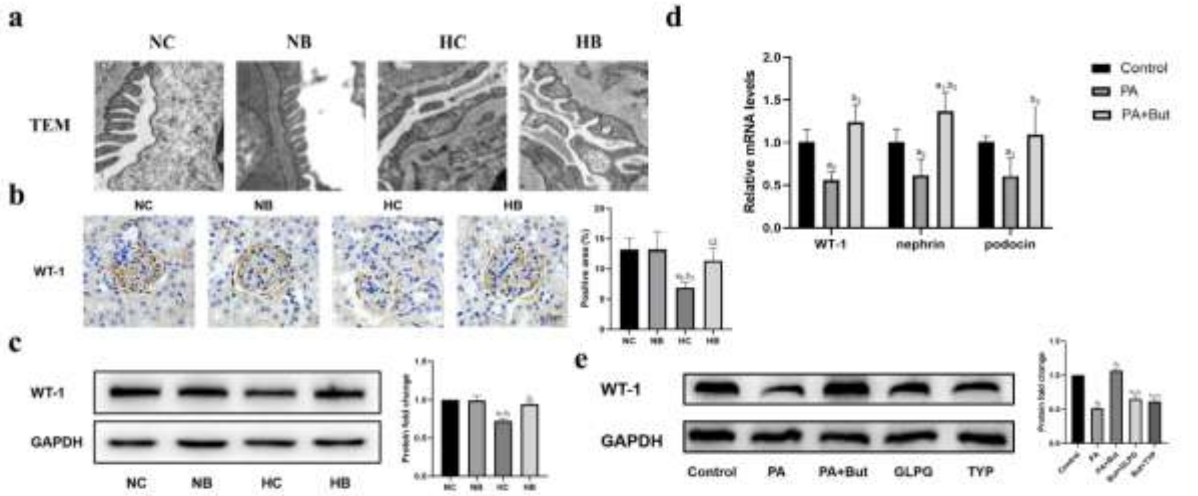

Figure 4. Sodium butyrate administration ameliorated HFD-induced podocytes damage. **(a)** TEM of podocyte foot processes and glomerular basement membrane in the kidney of mice treated with or without butyrate. Scale bars, 2μm. n=6 each group. **(b)** Immunohistochemistry assays and **(c)** Western blots assays for the expression of WT-1 in the renal cortex of mice treated with or without butyrate. n=6-8 each group. **(d)** Relative mRNA levels of WT-1, nephrin and podocin determined by RT-PCR in the MPC5 cells incubated with or without butyrate. **(e)** Western blots assays of WT-1 in the MPC5 cells incubated with or without butyrate, GLPG0974 or 3-TYP. TEM: Transmission electron microscopy; PA: palmitic acid; But: butyrate; GLPG: GLPG0974, the inhibitor of GPR43; TYP: 3-TYP, the inhibitor of Sirt3. All values are shown as the means ± SEM. **(b-c)** $^{a1}p<0.05$, $^{a2}p<0.01$ *vs.* NC group; $^{b1}p<0.05$, $^{b2}p<0.01$ *vs.* NB group; $^{c1}p<0.05$, $^{c2}p<0.01$ *vs.* HC group. **(d-e)** $^{a1}p<0.05$, $^{a2}p<0.01$ *vs.* Control group; $^{b1}p<0.05$, $^{b2}p<0.01$ *vs.* PA group; $^{c1}p<0.05$, $^{c2}p<0.01$ *vs.* PA+But group. Statistical significances were determined by one-way ANOVA.

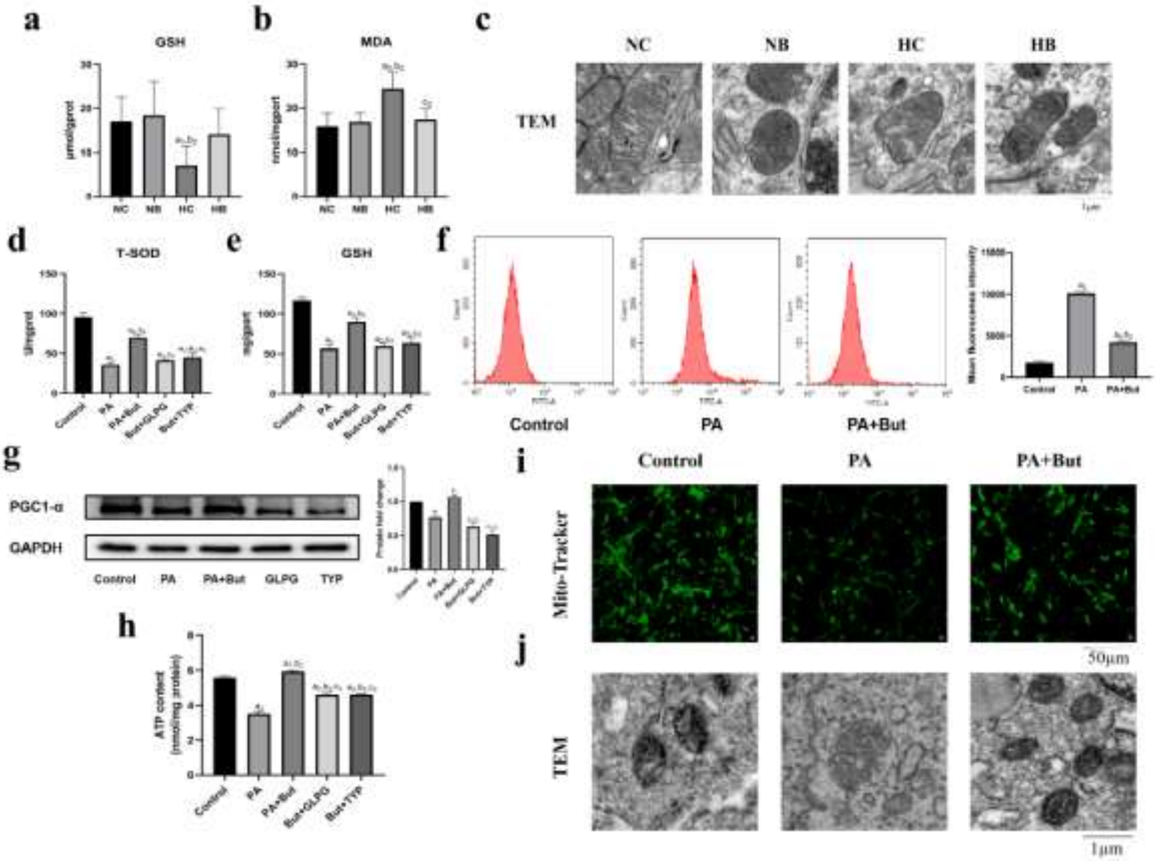

Figure 5. Sodium butyrate partially reversed HFD-induced oxidative stress and mitochondrial damage. **(a)** GSH and **(b)** MDA content in the kidney of mice treated with or without butyrate. n=6-8 each group. **(c)** TEM of mitochondrial morphology in the kidney of mice treated with or without butyrate. Scale bars, 1μm. n=6 each group. **(d)** T-SOD and **(e)** GSH content in the MPC5 cells incubated with or without butyrate, GLPG0974 or 3-TYP. **(f)** Cellular ROS production was detected by flow cytometry after DCFH-DA staining. **(g)** Western blots assays of PGC1-α in the MPC5 cells incubated with or without butyrate, GLPG0974 or 3-TYP. **(h)** ATP content in the MPC5 cells incubated with or without butyrate, GLPG0974 or 3-TYP. **(i)** Mitochondria were stained by MitoTracker Green and imaged by fluorescence microscope. Scale bars, 50μm. **(j)** TEM of mitochondrial morphology in the MPC5 cells incubated with or without butyrate. Scale bars, 1μm. GSH: glutathione; MDA: malondialdehyde; T-SOD: total superoxide dismutase; TEM: Transmission electron microscopy. PA: palmitic acid; But: butyrate; GLPG: GLPG0974, the inhibitor of GPR43; TYP: 3-TYP, the inhibitor of Sirt3. All values are shown as the means ± SEM. **(a-b)** $^{a1}p<0.05$, $^{a2}p<0.01$ *vs.* NC group; $^{b1}p<0.05$, $^{b2}p<0.01$ *vs.* NB group; $^{c1}p<0.05$, $^{c2}p<0.01$ *vs.* HC group. **(d-f, h)** $^{a1}p<0.05$, $^{a2}p<0.01$ *vs.* Control group; $^{b1}p<0.05$, $^{b2}p<0.01$ *vs.* PA group; $^{c1}p<0.05$, $^{c2}p<0.01$ *vs.* PA+But group. Statistical significances were determined by one-way ANOVA.

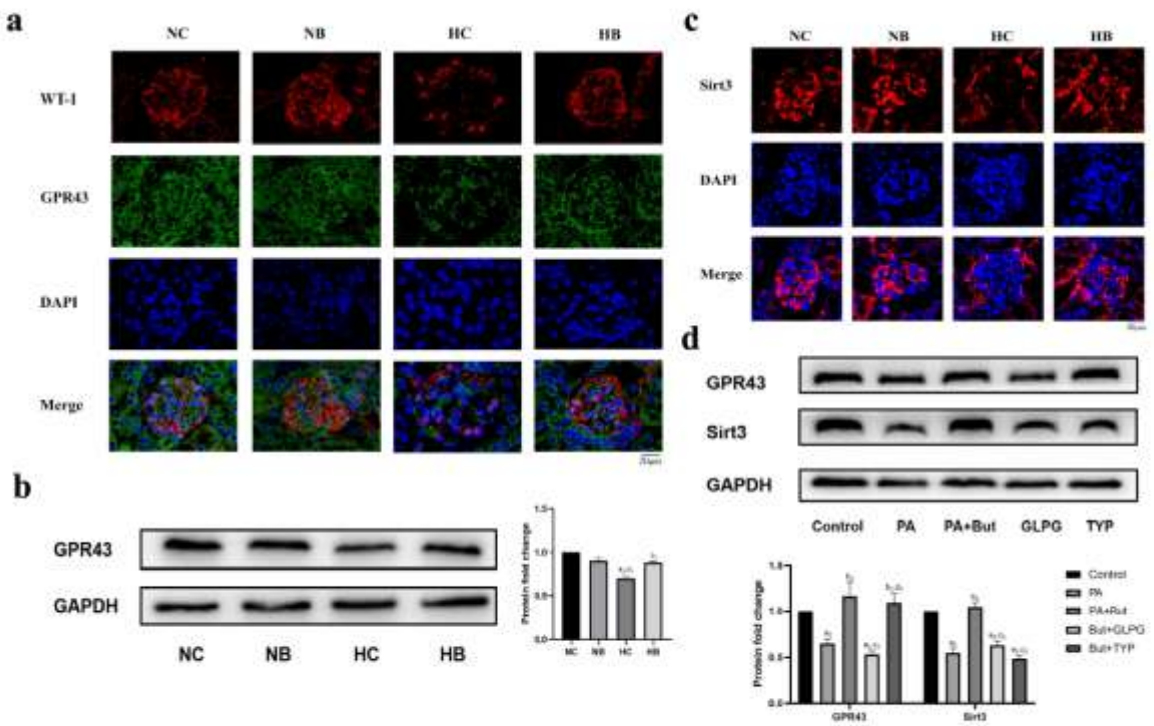

Figure 6. Sodium butyrate ameliorated podocytes injury via the activation of GPR43-Sirt3 pathway. **(a)** Immunofluorescence of kidney sections stained with WT-1 (red) and GPR43 (green). Nuclei were counterstained with DAPI (blue). Scale bars, 20μm. n=6 each group. **(b)** Western blots assays for the expression of GPR43 in the renal cortex of mice treated with or without butyrate. n=6-8 each group. **(c)** Immunofluorescence of kidney sections stained with Sirt3 (red). Nuclei were counterstained with DAPI (blue). Scale bars, 20μm. n=6 each group. **(d)** Western blots assays of GPR43 and Sirt3 in the MPC5 cells incubated with or without butyrate, GLPG0974 or 3-TYP. PA: palmitic acid; But: butyrate; GLPG: GLPG0974, the inhibitor of GPR43; TYP: 3-TYP, the inhibitor of Sirt3. All values are shown as the means ± SEM. **(b)** $^{a1}p<0.05$, $^{a2}p<0.01$ *vs.* NC group; $^{b1}p<0.05$, $^{b2}p<0.01$ *vs.* NB group; $^{c1}p<0.05$, $^{c2}p<0.01$ *vs.* HC group. **(d)** $^{a1}p<0.05$, $^{a2}p<0.01$ *vs.* Control group; $^{b1}p<0.05$, $^{b2}p<0.01$ *vs.* PA group; $^{c1}p<0.05$, $^{c2}p<0.01$ *vs.* PA+But group. Statistical significances were determined by one-way ANOVA.